Physical and Biological Controls on Carbon Cycling in the Equatorial Pacific

James W. Murray,* Richard T. Barber, Michael R. Roman, Michael P. Bacon, Richard A. Feely

The equatorial Pacific is the largest oceanic source of carbon dioxide to the atmosphere and has been proposed to be a major site of organic carbon export to the deep sea. Study of the chemistry and biology of this area from 170° to 95°W suggests that variability of remote winds in the western Pacific and tropical instability waves are the major factors controlling chemical and biological variability. The reason is that most of the biological production is based on recycled nutrients; only a few of the nutrients transported to the surface by upwelling are taken up by photosynthesis. Biological cycling within the euphotic zone is efficient, and the export of carbon fixed by photosynthesis is small. The fluxes of carbon dioxide to the atmosphere and particulate organic carbon to the deep sea were about 0.3 gigatons per year, and the production of dissolved organic carbon was about three times as large. The data establish El Niño events as the main source of interannual variability.

Because of the upwelling of CO_2-rich deep water, the central and eastern equatorial Pacific Ocean is the largest natural ocean source of CO_2 to the atmosphere [about 0.9 gigatons (Gt) of carbon per year (*1*)]. New biological production (production driven by the import of new nutrients to the euphotic zone) in this region could account for as much as 25 to 50% of the global ocean value (*2*). This view that the region has large carbon fluxes must be reconciled with the recent realization that the region is an example of a high nutrient–low chlorophyll (HNLC) regime. Physical and chemical distributions are dominated by upwelling, and surface waters usually have high concentrations of dissolved nutrients and high biological productivity. Phytoplankton biomass and productivity levels, although high, are lower than expected and have relatively small seasonal variability (*3*). The dynamics of this region are complex but have been reasonably well described (*4*). The upwelling has a large interannual variability associated with the El Niño–Southern Oscillation (ENSO); thus, carbon fluxes strongly depend on climate variability.

In order to determine the relative importance of physical versus biological processes in the control of the variability of concentrations and fluxes, the equatorial Pacific Ocean was chosen as the site of a U.S. Joint Global Ocean Flux Study (U.S. JGOFS) process study (*5*). The purpose was to determine the fluxes of carbon and related elements between the euphotic zone and the atmosphere and deep ocean. Pelagic studies principally addressed the mechanisms that make the equatorial Pacific an HNLC regime and the factors that control new and export production (*6*). In this article, we compare carbon fluxes with physical forcing on different time scales and discuss their control by the structure of the biological food web.

Dominant time scales range from interannual (ENSO) through seasonal and intraseasonal (Kelvin and instability waves) to diurnal (*7*). Space scales range from the depth of the mixed layer to the scale of the Pacific Basin. We planned cruises to observe these ranges of variability (*8*). Data on a comprehensive set of hydrographic, chemical, and biological parameters were collected during two field seasons from process-oriented survey cruises from 12°N to 12°S at 140°W and during 20-day time-series cruises at the equator at 140°W (*9*). A regional survey was conducted in each season along four meridional sections from 170°W to 97°W. We summarize here work conducted during February to May and August to October 1992. Figure 1 shows the results from these cruises. The cruises that took place during the February to May season (series I) coincided with the maximum intensity of the warm El Niño event, and the August to October cruises (series II) took place during well-developed cool surface water or "cold-tongue" conditions (*10*).

Carbon Dioxide

The high degree of supersaturation of CO_2 in surface water at the equator is the result of upwelling of CO_2-rich waters. Some of the upwelled CO_2 is biologically cycled within the euphotic zone, and some is released to the atmosphere, but most is transported away from the site of upwelling by advection.

The average annual increase of CO_2 in the atmosphere has been estimated to be about 1.4 parts per million (ppm) per year; however, the year-to-year increase fluctuates about the mean by about ±0.6 ppm $year^{-1}$ (*11*). Interannual variations in the rate of release of CO_2 by the surface of the equatorial Pacific appear to influence the rate of increase of atmospheric CO_2. The variations with the largest magnitudes coincide with El Niño events. When the atmospheric data are detrended for seasonal cycles, the rate of increase shows a minimum during the early phase of an El Niño followed by a maximum thereafter (*11*). For example, in the fall of 1982, during the early part of the 1982–1983 El Niño, the rate of increase of atmospheric CO_2 decreased to essentially zero [0.0 ± 0.3 ppm $year^{-1}$ (*1*)]. At the same time, the calculated gas exchange flux of CO_2 from the surface water of the equatorial Pacific (10°N to 10°S; 80°W to 135°E) to the atmosphere decreased from normal values of about 0.9 Gt of carbon per year to a negligible flux of less than 0.02 Gt C $year^{-1}$ (*12*). In the year following the 1982–1983 El Niño, atmospheric CO_2 grew at an anomalously high rate. The maximum rate of increase (2.2 ppm $year^{-1}$) occurred in early 1984 (*1*). This sequence of events appears to be characteristic of other El Niño events as well (*13*).

The simplest explanation of the connection is that the CO_2 content of the surface eastern equatorial Pacific is reduced during the first part of an El Niño, when Kelvin waves depress the thermocline, because the mixed layer waters that replace the thermocline as it moves downward have much less CO_2. Upwelling continues during El Niño events, although reduced in proportion to wind strength, and the water upwelled is warmer and has less CO_2. The end of an El Niño event is associated with re-establishment of the upwelling of cold CO_2-rich waters, which gives rise to the high CO_2 concentrations usually observed and higher fluxes to the atmosphere. The terrestrial biosphere is also involved (*14*). Keeling *et al.* (*15*) used atmospheric $\delta^{13}C$ measurements to argue that the increase in atmospheric CO_2 levels after an El Niño event was primarily the result of reduced uptake

---

J. W. Murray is with the School of Oceanography, University of Washington, Seattle, WA 98195, USA. R. T. Barber is with Duke University Marine Lab, Beaufort, NC 28516, USA. M. R. Roman is with Horn Point Environmental Lab, University of Maryland, Cambridge, MD 21613, USA. M. P. Bacon is with Woods Hole Oceanographic Institution, Woods Hole, MA 02543, USA. R. A. Feely is with Pacific Marine Environmental Lab, 7600 Sand Point Way, NE, Seattle, WA 98115, USA.

*To whom correspondence should be addressed.

by terrestrial vegetation resulting from drought conditions caused by the collapse of the southeast Asian monsoon (*16*). There is some uncertainty, however, and not all atmospheric $\delta^{13}C$ data are consistent with this notion. From the middle of 1991 to 1993, the rate of increase in atmospheric CO_2 was drastically reduced from its normal value of about 3 Gt C year^{-1} to about 1 Gt C year^{-1} (*17*). Atmospheric CO_2 began to increase at a faster rate in 1994, similar to that in 1984.

The fugacity of CO_2 (f_{CO_2}) in surface seawater from 110° to 170°W during the 1992 El Niño was generally lower than during previous non–El Niño periods. These data indicate that the nature of water upwelled at the equator changed (*18*). The values of f_{CO_2} during the El Niño ranged from 335 to 365 μatm along 170°W. The f_{CO_2} minimum at the equator was the result of an eastward advection of a low-salinity equatorial surface jet, which was observed as a shallow salinity minimum from about 2°S to 2°N at 170°W. This lower density water mass formed a cap that inhibited the upwelling of CO_2-enriched water. Near the edges of this jet (3°N and 3°S), deeper water upwelled and the surface seawater was always supersaturated in CO_2. At 140°W, surface seawater was supersaturated with respect to the atmosphere from 10°S to 7°N, and f_{CO_2} ranged from 347 to 410 μatm.

The difference in the fugacity of CO_2 between surface seawater and the atmosphere (Δf_{CO_2}) for the region from 110° to 170°W (Fig. 2) resulted in gas exchange fluxes to the atmosphere that ranged from 1.0 to 2.1 mmol C m^{-2} day^{-1} (*18*). The distribution was asymmetrical, and the fluxes south of the equator were about twice the values to the north. The Δf_{CO_2} maximum at the equator appeared to be the result of shallow upwelling from a depth of approximately 40 to 80 m, on the basis of temperature, salinity, and total CO_2 distributions.

During the resumption of cold-tongue conditions in August to October, the Δf_{CO_2} maximum along 140°W was 15 to 25 μatm higher than in February to May (Fig. 2). The calculated CO_2 gas exchange fluxes between 140° and 95°W for this period averaged 3.8 mmol C m^{-2} day^{-1} (*18*). Similar values were calculated for previous non–El Niño conditions (*12*, *19*). Farther to the east, along the 110°W transect, the Δf_{CO_2} maximum was as much as 55 μatm greater than in the spring. The higher surface f_{CO_2} during this period occurred because the nutricline (the depth at which the concentration of nutrients increases sharply) was shallower. The total flux to the atmosphere for October 1991 to September 1992 for the region 10°N to 10°S and 80°W to 135°E was 0.3 Gt year^{-1} (*18*). The net annual decrease in the CO_2 flux from the ocean to the atmosphere for this region was about 0.6 Gt C year^{-1}. The rate of increase in atmospheric CO_2 decreased by 2 Gt C year^{-1}, suggesting that the decreased flux of CO_2 from the equatorial ocean accounts for about 30% of the atmospheric anomaly.

Physical Forcing

In general, the circulation in the equatorial Pacific can be characterized as a vigorous meridional recirculation of water and nutrients in the upper 100 m from the equator to about 5°N and 5°S, superimposed on deeper zonal transport from the west, which introduces new nutrients and is associated with the equatorial undercurrent. The fluxes of CO_2 to the atmosphere and particulate carbon to the deep

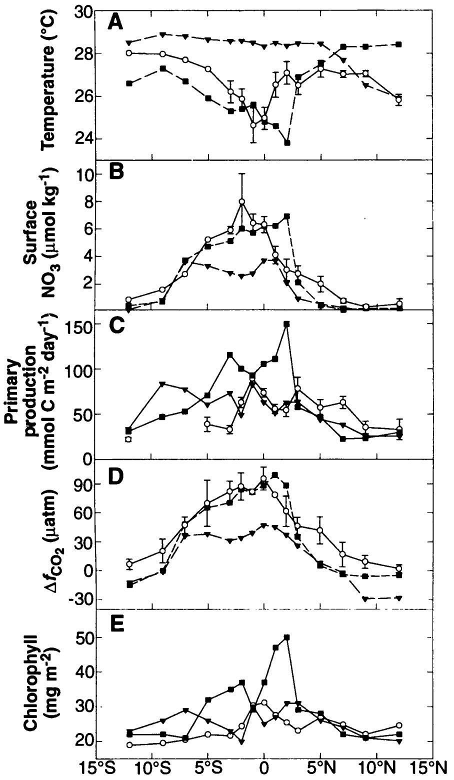

Fig. 1. Comparison of data from the R/V *Thompson* survey I (February to March 1992) (▼) and survey II (August to September 1992) (■) cruises with the average of previous determinations (climatology) (○) calculated by Barber and Chavez (*79*). The data correspond to meridional transects from 12°N to 12°S along 140°W. (**A**) Surface temperature, (**B**) surface nitrate (*80*), (**C**) integrated primary production to the 0.1% light level, (**D**) Δf_{CO_2} (*42, 81*), and (**E**) integrated chlorophyll to 120 m.

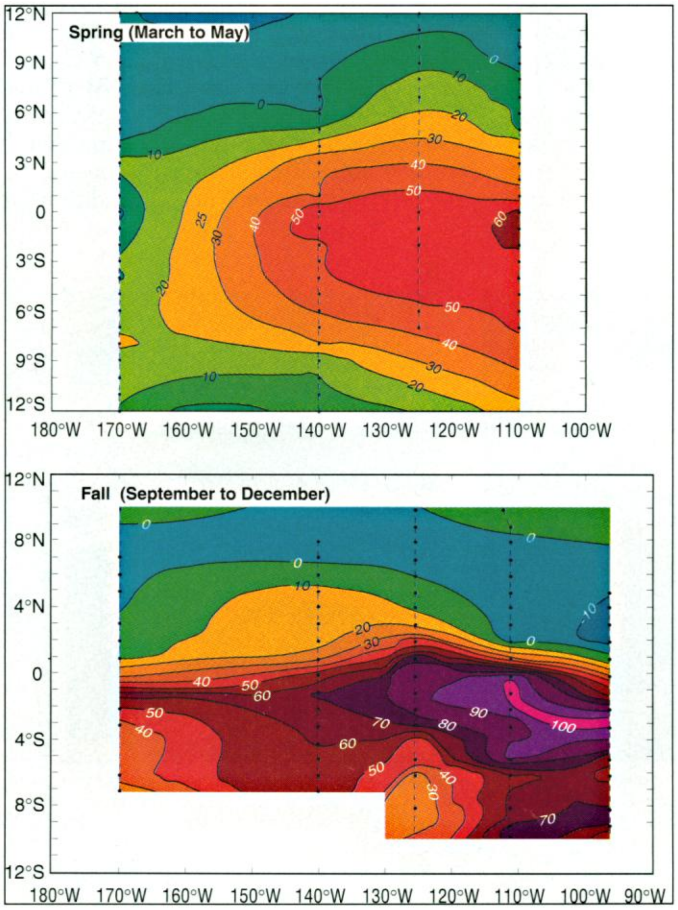

Fig. 2. Maps of the distribution of Δf_{CO_2} (ocean − atmosphere) (in microatmospheres) for surface seawater from 10°N to 10°S and 170°W to 95°W for February to May and September to December 1992. Data obtained from the NOAA cruises on the R/V *Baldridge* and R/V *Discoverer* (*18*).

ocean depend not only on biological processes like primary production, grazing, and export, but also on physical processes, including horizontal advection, changes in upwelling rates, and wind speed. It is necessary to understand the relative importance of remote versus local physical forcing in order to evaluate the controls on the larger scales of temporal and spatial variability.

The warm event that reached maximum intensity in early 1992 began in September 1991 as a series of westerly wind events lasting about 30 days each that occurred primarily west of the date line over the western Pacific warm pool (Fig. 3A) (*20*). Each wind event excited an eastward propagating equatorial Kelvin wave that carried the downwelling signal of the westerly winds to the eastern Pacific (*21*). As a result, there were large and rapid changes in the depth of the thermocline in the central equatorial Pacific; for example, it dropped as much as 50 m in one week at 140°W in late January (Fig. 3B). The importance of the remote Kelvin wave forcing is demonstrated by the fact that the depth of the 20°C isotherm at 140°W was highly correlated with zonal winds at 165°E (*22*) but not at all with local winds. It is notable that the 20°C isotherm at 140°W reached its deepest level during the event at the end of December 1991, before any local wind anomalies occurred (Fig. 3).

The surface-water cold tongue was absent at 140°W during the survey I cruise (February) (Figs. 1A and 4A), even though easterly winds were strong. With the exception of 2-week periods in January and April, the local zonal winds at and east of 140°W were near or slightly stronger than normal throughout the entire year (Fig. 3A), although in general, easterly winds were stronger between August and October than they were between February and May. Winds favored upwelling through nearly all of 1992 at 140°W despite the anomalously high sea surface temperatures (SSTs) for much of the time. Strong horizontal divergence and upwelling appear to be concentrated in a narrow band 20 km wide centered on the equator (*23*). Semiannual variations of upwelling velocity are substantial and are in phase with local wind forcing (Fig. 3). The relation between zonal wind strength and the depth of the water upwelled to the surface is complex, but the conventional view is that the path of most of the upwelled water is along isopycnal surfaces that outcrop at the equator and deepen to between 50 and 100 m north and south of the equator (*24*). As a result, the remote winds in the western Pacific, which control the depth of the local thermocline, also control the properties of the upwelled water (*20*). Temperature sections from 12°N to 12°S along 140°W (Fig. 4) suggest that the source of upwelled water tended to be shallow (40 to 80 m) from February to May and slightly deeper from August to October. The distributions of other hydrographic and nutrient properties are consistent with this view. Because the thermocline was depressed to deeper than 100 m from February to May, the upwelled water was warm (28.5°C) and relatively nutrient-rich (Fig. 1B) (Table 1). Water with a temperature of 28.5°C and a nitrate concentration greater than 3 μM is unusual in the world's oceans.

After our survey I cruise conditions at 140°W started to change toward normal conditions during our time series I and the National Oceanic and Atomspheric Administration's (NOAA's) survey I cruises (April). The maximum SST at 140°W occurred at the end of March and was still 2°C above normal during April. On the other hand, the depth of the 20°C isotherm anomalies at 140°W was zero by the end of April. During April the conditions were still anomalous [SST and depth of the 20°C isotherm (Fig. 3B)], but the anomalies were decaying. These rapid changes in the physical regime make it difficult to compare chemical and biological data from different cruises, even in the same season.

A well-developed cold tongue was reestablished at the equator by June, so the SSTs during the survey II (August) (Figs. 1A and 4), time series II (October), and NOAA survey II (September) cruises were equal to or slightly colder than normal. However, SSTs remained anomalously warm north and south of the equator. Tropical instability waves were well developed during the second half of 1992 compared with those in previous years. The tropical instability waves are associated with 20- to 30-day fluctuations of the meridional currents between the equator and 5°N and lead to large oscillating meridional advection of upper layer water properties. The cold phase was of short duration, yet all our cruises sampled the equator before warm conditions reintensified in March 1993. The warm event ended at the end of 1993 (*25*).

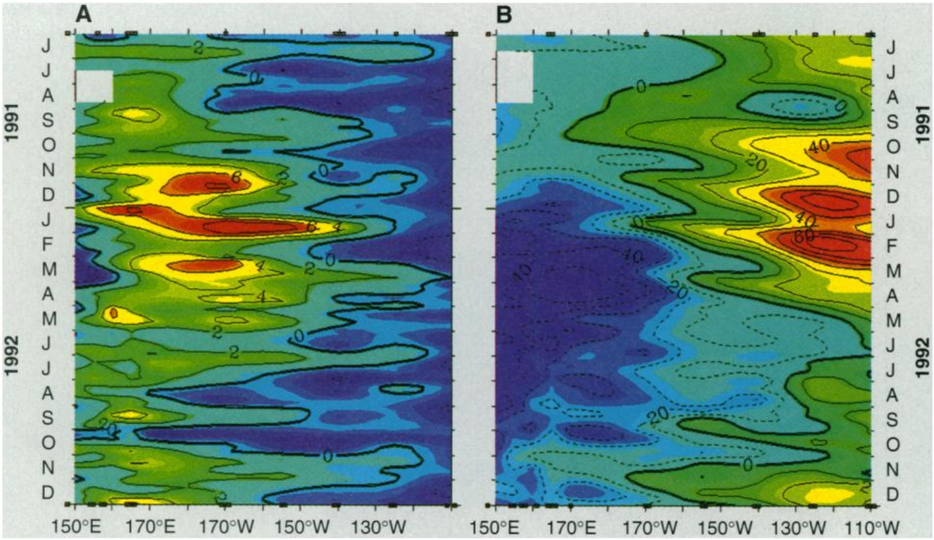

Fig. 3. (**A**) Zonal wind anomalies (in meters per second) and (**B**) anomalies of the depth of the 20°C isotherm (in meters) for June 1991 to December 1992 for the equatorial Pacific from 150°E to 110°W determined from the TOGA-TAO moored array (*10*). The heavy line in both figures represents the zero anomaly boundary.

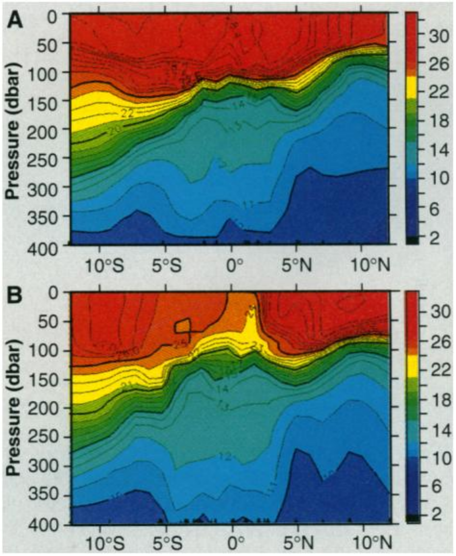

Fig. 4. Meridional sections of potential temperature (in degrees Celsius) varying with depth (100 dbar ≈ 100 m) from 12°N to 12°S at 140°W during (**A**) survey I (4 February to 9 March 1992) and (**B**) survey II (9 August to 16 September 1992) cruises.

Previous Modeling Results

Several modeling studies influenced the design of our field program. Najjar *et al.* (*26*) added a phosphate mass balance equation to an ocean general circulation model and concluded that dissolved organic matter needed to be a major form of the export production in order to prevent positive feedback from resulting in excessively large upwelled nutrient concentrations. They predicted export production of 5 to 15 mmol C m^{-2} day^{-1}, depending on the depth dependence of the particle remineralization rate. Best agreement between model and observed data was obtained when most of the export of organic matter took place in a dissolved phase. Siegenthaler and Sarmiento (*27*) characterized global export production as 60% dissolved organic carbon and 40% particulate organic carbon.

This approach was developed further with a more extensive coupled physical-ecological model. The model coupled a highly resolved description of the tropical Pacific circulation field (*28*) with a seven-compartment ecosystem model (*29*). The results (*30*) suggested that (i) surface nutrients and biomass were asymmetrically distributed toward the southern hemisphere, (ii) the dominant variability near the equator was produced by 20- to 30-day tropical instability waves, (iii) recycled ammonia from the single grazer in the model was responsible for keeping nitrate uptake at relatively low levels, and (iv) if there is a long-lived pool of dissolved organic matter, it would be a major advective export of carbon out of the equatorial region. The role of grazing was further elucidated by Frost and Franzen (*31*), who used a simple chemostat analog model to show that both herbivore and carnivore grazers and preferential uptake of ammonia over nitrate by phytoplankton were required to reproduce observed nutrient and biomass values.

Variability in Biological Parameters

Comparison of the cruise results at the equator at 140°W reveals low-frequency variability (Table 1). Water that upwelled to the euphotic zone at the equator was warm and relatively nutrient-rich (*32*) between February and May and cool and nutrient-rich from August to October (Fig. 1B) (Table 1). Barber and Chavez (*33*) defined water with nitrate concentrations over 4 μM as nutrient-rich. During both periods, the distributions were asymmetrically distributed toward the southern hemisphere.

The chemical and biological differences were subtle, considering the large differences in the SST and nutrients. Chlorophyll in the euphotic zone (*34*) varied little from 12°N to 12°S during survey I and tended to be about a factor of 2 higher from 2°N to 5°S during survey II (Fig. 1E). The chlorophyll inventories at the equator were 50% higher during survey II compared with those during survey I and 14% higher during time series II compared with those during time series I (Table 1). Primary production determined by ^{14}C analysis was maximum near the equator and had asymmetrically high values south of the equator during both seasons (Fig. 1D) (*35*). Primary production increased significantly from survey and time series I to survey and time series II (Fig. 1C and Table 1). Some of the increase was caused by an increase in biomass. In addition, the specific rate of primary production was about 25% higher during time series II compared with that during time series I (*32*).

It is not clear yet what explains these differences, but changes in nutrients (including iron), light, and plankton community structure are likely candidates. There were a few very cloudy days with heavy rain during time series I, but even with these occasional cloudy days removed, time series I was still less productive than time series II. Another possible cause of the difference was the larger magnitude of diurnal changes in mixed-layer depth in time series II (from 10 to 70 m) compared with those in time series I (from 5 to 35 m) (*36*). Changes in the composition of the primary producers and the effect of these changes on grazing losses were probably the direct cause of the increase in primary production.

Coherent, high-frequency variability was observed in the results from the time series cruises. Time series I was a relatively stable period with little systematic variability in the observations. During time series II, however, there were coherent high-frequency changes in the magnitude of meridional and zonal currents, reflecting the passage of a tropical instability wave and resulting in large changes in temperature, salinity, nutrients, chlorophyll, and primary production (Fig. 5). There was also an increase in mesozooplankton biomass associated with the instability wave, although the increase lagged behind the increase in nutrients and chlorophyll. The maximum nitrate and chlorophyll concentrations and minimum temperature were associated with the maximum northward current velocity (*10*). Primary production also peaked with nitrate and chlorophyll levels, but when productivity was normalized to chlorophyll, the specific rates did not change (Fig. 5B) (*37*). This indicates that the increase in primary production was controlled by variations in biomass rather than changes in the specific biological rates. When biomass

Table 1. Variability in hydrographic, chemical, and biological parameters at the equator and 140°W during 1992. Integrated values are for the surface to the 0.1% light level, which is about 120 m, except where indicated.

	Survey I	Time series I	NOAA I	Survey II	NOAA II	Time series II
Dates (month/day)	2/23–2/25	3/23–4/10	4/30	8/28–8/31	9/15	10/1–10/21
SST (°C)	28.4 ± 0.2	28.6 ± 0.2	28.7 ± 0.2	24.9 ± 0.2	25.5 ± 0.2	25.1 ± 0.3
Depth of 20°C (m)	122 ± 9	119 ± 10	85 ± 5	101 ± 6	94 ± 5	113 ± 12
Surface NO_3 (μmol kg^{-1}) (*80, 82, 83*)	3.0 ± 0.2	2.9 ± 0.2	3.0 ± 0.5	6.1 ± 0.4	3.8 ± 1.5	5.9 ± 0.9
Integrated chlorophyll (mg m^{-2}) (*34, 62, 87*)	25.1 ± 2.2	29.3 ± 2.6	29.3	36.5 ± 4.8	25.7	33.5 ± 6.7
Biomass (mmol C m^{-2})						
Integrated phytoplankton from C:Chl = 58	120	140	140	178	124	164
Integrated bacterial (*84*)	93	96		114		122
Heterotrophic nanoplankton (*51*)	18.1	53.2		66.7		57.8
Bacterial/phytoplankton biomass	0.77	0.68		0.64		0.74
Primary production (mmol C m^{-2} day^{-1}) (*35, 87*)	63	90	99*	105	104*	129
Bacterial production (mmol C m^{-2} day^{-1}) (*84*)	10.2	18.8		13.3		17.9
Bacterial/phytoplankton production	0.16	0.21		0.13		0.14
Integrated mesozooplankton biomass (mmol C m^{-2}) (>200 μm) (*74, 85*)	33.3	21.8		31.4		33.9
Δf_{CO_2} (μatm) (*18, 42, 86*)	45.0	57.0	55	83.0	65	90

*To the 1% light level.

is controlled by grazing, the specific growth rate should be independent of biomass. The reason why biomass was higher in the cool, nitrate-rich water even though nitrate was always greater than 4.5 μM was probably because there was less grazing during the water's previous history.

The variability associated with instability waves can also be seen in zonal transects along the equator. Lefevre and Dandonneau (*38*) showed that Δf_{CO_2} along the equator in the eastern equatorial Pacific in January to March, 1991, exhibited a large variability as a result of tropical instability waves. In May 1992, during a NOAA transect from 130° to 100°W (*39*), temperature was inversely related to salinity, density, nitrate, and carbonate system parameters (pH, total alkalinity, total CO_2, and f_{CO_2}) (Fig. 6). The data show that temporal variability of hydrographic, chemical, and biological data at a given point on the equator can be quite large.

Another example of the physical control of the biological distributions associated with tropical instability waves was the frontal feature and associated *Rhizosolenia castracanei* patch at 2°15′N, 140°W observed during the survey II cruise (*40*). The front was a boundary between cold (23.8°C) and warm (25.0°C) water on the western side of the crest of a tropical instability wave traveling with a velocity of about 30 km day^{-1}. Acoustic doppler current meter data showed strong convergence and downwelling (*41*). Linear features related to this instability wave are also present in photographs taken from the space shuttle Atlantis (*40*). *Rhizosolenia* is a large, buoyant, chain-forming diatom that was present in the region and was concentrated into a dense surface patch by convergence at the front. This patch was not a bloom but an accumulation driven by the advective concentration effects of the convergent front. Although surface chlorophyll concentrations in the patch reached 10 to 30 mg m^{-3}, specific biological growth rates (P^B_{max} equaled 90 mg of carbon per milligram of chlorophyll per day) were similar to those in the region away from the front (Fig. 5B). The large increase in biomass and total production resulted in a local CO_2 depletion with Δf_{CO_2} decreasing from +90 μatm south of the front to −19 μatm in the patch north of the front (*42*).

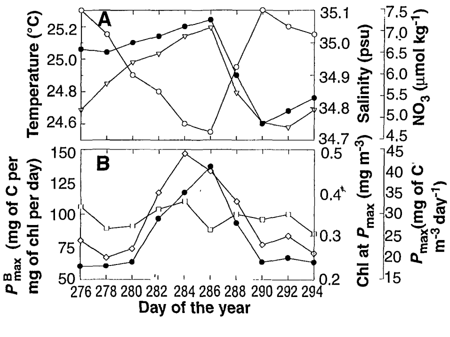

Fig. 5. (**A**) Physical [temperature (○) and salinity (●)] and chemical [nitrate concentration (▽)] (*82*) and (**B**) biological [P^B_{max} (□), chlorophyll concentration at depth of P_{max} (●), and P_{max} (◇)] data from the NSF R/V *Thompson* time series II (October 1992) cruise at the equator and 140°W. P_{max} is the maximum value of primary production in the vertical profile; P^B_{max} is the ratio of primary productivity to chlorophyll and is shown for the depth of maximum productivity.

The determinations of dissolved organic carbon (DOC) made during cruises in this study (*43*) substantiated previous model calculations that DOC may be a significant form of export production from the equatorial Pacific (*26*, *44*). In general, surface (0 to 100 m) DOC values increased from 60 to 65 μmol of carbon per kilogram of water at the equator to about 70 μmol C kg^{-1} at 2°N and 2°S and to 80 μmol C kg^{-1} at 12°N and 12°S (*45*). Zonal variability was small. The DOC concentrations typically decreased from the high surface values to about 45 μmol C kg^{-1} at 200 m. This result suggests that DOC was produced in the euphotic zone and consumed just below in the thermocline. Data from the meridional sections suggest that water with relatively low DOC content was upwelling near the equator. Production of DOC resulted in increased concentrations as the water was advected to the north and south.

Food Web Considerations

The flux of carbon, nitrogen, and other biogenic elements within and out of the euphotic zone is a function of food web structure. Previous studies of HNLC regimes have indicated that nano- and picoplankton are dominant primary producers and are tightly coupled to an active community of protozoan grazers. These regimes typically have low values of new and export production. The data from the equatorial Pacific are consistent with these observations (Table 2).

The bulk plankton community during both the I and II series cruises was dominated by picoplankton. The fraction of the chlorophyll in the <2-μm size fraction was 92% during time series I and 81% during time series II. Larger plankton, expressed as chlorophyll in the >14-μm fraction, were more abundant during time series II (*46*). Prochlorophytes and cyanobacteria were significant components of the phytoplankton biomass during all cruises, but eukaryotic phytoplankton (especially diatoms) were more abundant during time series II (*46*, *47*). Significant increases of stepped-chain and cluster-forming diatom species of *Pseudonitzschia delicatissima* and large single diatoms *Thalassiothrix* and *Thalasssionema* (*48*) were observed during survey II and time series II. The percent of chlorophyll attributed to diatoms increased from <0.1 to 6% between survey I and survey II (*49*).

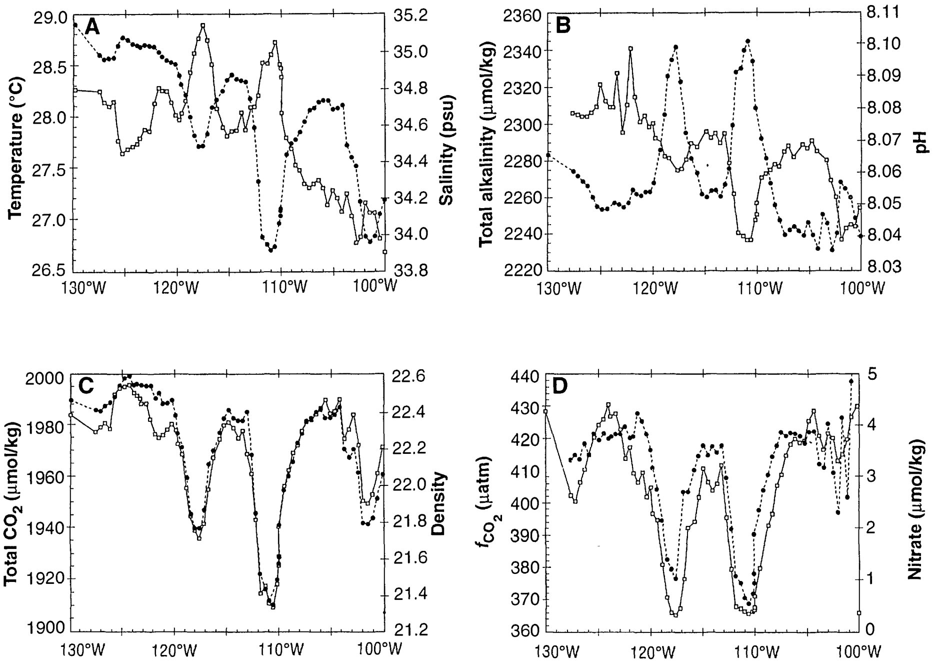

Fig. 6. Data from the NOAA R/V *Discoverer* cruise in May 1992 along the equator from 130° to 100°W. These results illustrate the variability caused by the tropical instability waves. The data have an apparent 700-km wavelength and a 15-day period. The real dimensions are longer because the ship and waves were traveling in opposite directions. Values are given for (**A**) temperature (□) and salinity (●), (**B**) total alkalinity (□) and pH (●), (**C**) total CO_2 (●) and density (σ_T) (□), and (**D**) fugacity of CO_2 (●) and nitrate (□) (*39*).

Total phytoplankton biomass was 14% lower during time series I relative to time series II. El Niño conditions appear to result in a small reduction in the phytoplankton biomass, especially in the eukaryotic phytoplankton (prymnesiophytes, chrysophytes, and diatoms).

Modeling studies summarized earlier suggest that more than one size of grazer is necessary to reproduce the nutrient and biomass conditions. A steady-state balance between the production of biomass by phytoplankton and its consumption by two size classes of grazers, such as microzooplankton and mesozooplankton, grazing at a rate g (per day), can be written as

$$\mu_{\mathrm{phyto}} = g_{\mathrm{micro}} + g_{\mathrm{meso}} + \text{nongrazing losses}$$

Grazing by microzooplankton was tightly coupled to the primary production; the grazing rates of the microzooplankton were close to the growth rates of the phytoplankton (50). For example, during survey I the average phytoplankton growth rate at depths of 10 to 80 m at the equator was 0.46 day^{-1}, and the microzooplankton grazing rate was 0.38 day^{-1}. During survey II, when the primary production was higher, there was more of an imbalance between mean phytoplankton growth (0.77 day^{-1}) and microzooplankton grazing (0.42 day^{-1}). The production-grazing system may have been uncoupled because of the changing physics. Similar rates were measured during the time series cruises (51). Grazing of phytoplankton by microzooplankton represents a major transformation of organic carbon during both El Niño and cold-tongue conditions. The shift in community structure during the cold tongue to include more large diatoms is consistent with decreased grazing impact by microzooplankton.

One of the main trophic roles of microzooplankton is to serve as food for large grazers. Mesozooplankton biomass in the euphotic zone increased from time series I to time series II (Table 1), but their grazing impact, expressed as removal of chlorophyll production, actually decreased from 8.3 to 4.0% (52). It appears that mesozooplankton biomass in the equatorial Pacific is low relative to primary production, but there have been few studies of other regions upon which to base a predictive relation (53). The coincidence of higher mesozooplankton biomass with higher primary production during the cold-tongue period suggests that primary production limits the biomass of this larger, longer lived heterotrophic group.

Previous studies of HNLC regimes, including the equatorial Pacific, have revealed low values of new production (54–58), consistent with a microzooplankton-dominated food web. New production is usually approximated by the NO_3^- uptake rate (ρ_{NO_3}) and regenerated production by the ammonia uptake rate (ρ_{NH_4}). Dugdale *et al.* (56) found that the rate of NH_4^+ uptake was two to six times higher than NO_3^- uptake, and the resulting turnover times in the euphotic zone averaged 197 days for NO_3^- and 1 day for NH_4^+. Given the average meridional advective time scales in the equatorial region (~10 km day^{-1}), the average NO_3^- molecule will travel far from the zone of upwelling before it is taken up. Ammonium depresses utilization of nitrate and may be preferentially taken up by phytoplankton (57, 59), although the exact nature of the interaction is uncertain (60). Elevated NH_4^+ concentrations, especially during survey I and time series I, may be a main reason why NO_3^- is not fully utilized (59). Because of the vigorous meridional recirculation cell and upwelling fed by water on isopycnal surfaces, upwelled NO_3^- may be subducted and upwelled again without being taken up and the upwelled water may also contain NH_4^+. Thus, the traditional approach for estimating new and regenerated production as a vertically driven system may have to be modified for this region.

Export production is also low in HNLC regions. Earlier measurements of the particulate organic carbon (POC) flux with the use of drifting sediment traps showed that export production in the eastern equatorial Pacific (85°W) was low, ~6 mmol C m^{-2} day^{-1} (54). The *e* ratio (defined as the POC flux at the base of the euphotic zone divided by the primary production) was about 0.20. Drifting trap measurements were made by Betzer *et al.* (61) in the central equatorial Pacific at 153°W, but the traps were at 900 m and measured mass rather than organic carbon flux. If 50% of the mass was organic matter, their organic carbon flux to 900 m at the equator was about 0.4 mmol C m^{-2} day^{-1}.

In this study, we estimated particulate export production using drifting sediment traps (62) and the ^{234}Th method (63–65). The drifting sediment traps were calibrated by comparison of measured and calculated fluxes of ^{234}Th (65). On this basis, it appears that the traps from 75 to 125 m collected too much material, whereas the traps from 150 m to 250 m showed little bias. The average near-equatorial POC flux at 120 m by the ^{234}Th-corrected trap approach equalled 3.2 mmol C m^{-2} day^{-1} during survey I and 11.4 mmol C m^{-2} day^{-1} during survey II (Table 2). The POC flux estimated by the ^{234}Th method (66) gave values of 2.8 to 2.9 mmol C m^{-2} day^{-1} (Table 2). The variability in the survey II fluxes was due to differences in the estimates of the C/^{234}Th ratios of sinking particles. In the equatorial region, the particulate export production was significantly lower than the new production (59), indicating that 60 to 90% of the new production was transported away from the equator

Table 2. Characteristics of the biological food web at the equator and 140°W during 1992.

	Survey I	Time series I	Survey II	Time series II
Chlorophyll a (%) (49)				
In <2-µm size fraction	87.8	92.3		81.2
In >14-µm size fraction	3.0	2.6		11.5
As diatoms	<0.1		6.2	
Mean phytoplankton growth rate (µ) from primary production and phytoplankton biomass (0 to 120 m)	0.53	0.64	0.59	0.79
Mean phytoplankton growth rate (µ) by dilution experiment (10 to 80 m) (50, 51)	0.46	0.56	0.77	0.82
Mean microzooplankton grazing rate (*m*) by dilution experiment (10 to 80 m) (50, 51)	0.38	0.38	0.42	0.65
Phytoplankton carbon production (%)				
Grazed by microzooplankton	83	73	55	78
Grazed by mesozooplankton (52)	12	5	2	3
Particulate carbon flux at 120 m (mmol C m^{-2} day^{-1})				
Drifting traps corrected using ^{234}Th (2°N–2°S) (62, 65)	3.2		11.4	
^{234}Th method (63, 65)	2.8	2.1	2.9	2.4
e Ratio (POC flux/primary production)	0.044	0.022	0.028	0.019

by currents, possibly as DOC. The independent estimates of new and export production agree, and the low values of both are indications that the coupled production-grazing-regeneration system must be extremely efficient and close to steady state.

Earlier model predictions that DOC was a major form of carbon cycling can now be evaluated because of recent improvements in analytical technique (*67*). Model predictions of DOC production at the equator depend on estimates of upwelling velocity. Unfortunately, estimates of upwelling velocity at the equator vary widely and depend strongly on the wind forcing used (*68*). Using an upwelling rate of 0.7 m day^{-1} (*69*), Feely *et al.* (*18*) estimated the rates of production of DOC in the upper 100 m to be 8 ± 3 mmol C m^{-2} day^{-1}. This value was as much as three times larger than the vertical sinking flux of POC and the CO_2 loss by gas exchange.

Processes controlling primary production (PP) can be expressed as

$$PP = \mu_{\text{phyto}}P$$

where μ_{phyto} (per day) is the phytoplankton growth rate, which is a function of light, nutrients, and phytoplankton species, and P (millimoles of carbon per liter) is the phytoplankton biomass, which is controlled primarily by grazing. Primary production during the period of the cold tongue was higher than it was during the warm period. The difference may be a result of changes in the species of phytoplankton present. More diatoms during time series II, with potentially higher growth rates, could explain the higher observed phytoplankton growth rates. Nutrient concentrations were higher during the cold-tongue period, but major nutrient concentrations were high enough during all cruises to saturate nutrient uptake. During the survey I cruise, the concentration of dissolved iron at the equator and 140°W ranged from less than 0.03 nM in the surface water to 0.30 nM just below the equatorial undercurrent (EUC) at about 200 m (*70*). The origin of the high iron in the EUC is unknown but may be from the region of New Guinea in the western Pacific where the EUC originates (*71*). Increased upwelling and a shallower EUC during the survey II cold-tongue period may have resulted in increased iron stimulating diatom growth and primary production. The EUC may be a larger source of iron than the atmosphere as originally argued by Martin (*72*).

The EqPac data (all cruises taken together) suggest that microzooplankton grazing controls on primary production were similar to those observed in the subarctic North Pacific at station P (*73*) and in the oligotrophic North Atlantic at station S (*74*). This is an intriguing comparison because neither the equatorial Pacific nor the subarctic Pacific is limited by macronutrients, although iron apparently plays some role in both regions. All nutrients are considered limiting at station S. At all three locations, the phytoplankton were dominated by small cells that, on the basis of their P^B ratio (primary productivity to chlorophyll), may have been growing at rates close to their physiological potential for specific temperature and light conditions. The high area-to-volume ratio of these small cells gives them a competitive advantage under conditions of low iron concentrations (*75*), but their biomass is maintained at fairly low, constant levels by micrograzers, which have growth rates similar to those of the phytoplankton and which can respond quickly to changes in biomass. Relatively high primary production rates are maintained on recycled nitrogen. Because of the rapid response of grazers to changes in phytoplankton in this balanced ecosystem, herbivore biomass production rate is likely controlled by the phytoplankton growth rate. Grazing, in turn, supports primary production by regenerating ammonia. Large phytoplankton (especially diatoms) grow at rates less than their maximum potential at equatorial iron levels, but they bloom with increases in iron supply because micrograzers cannot graze them and their growth rate exceeds the growth rate response of the macrograzers. Maximum quantum yield (ϕ_m), maximum change in quantum yield ($\Delta\phi_m$), and atmosphere aerosol iron input decrease from 12°N to 12°S, suggesting that iron availability may limit rates of photosynthesis and growth of the entire phytoplankton community (*76*).

Mass Balance Considerations

Physical processes operating on several time and space scales played an important role in determining the chemical and biological variability in the central equatorial Pacific during 1992. Physical forcing of the equatorial region, especially remote winds in the western Pacific, controlled much of the low-frequency chemical and biological variability by influencing the depth of the nutricline and thus the composition of the upwelled water. Much of the high-frequency variability of properties at a specific location was controlled by tropical instability waves.

The biological community is dominated by picoplankton and microzooplankton grazers, and the fraction of carbon exported, by either the vertical particle flux or DOC production, was relatively small. This result was surprising considering the strong biogenic signal in the underlying sediments (*77*). Both grazing control and preferential utilization of ammonia by phytoplankton (*59*) are required to explain the concentrations of nitrate and ammonium in the euphotic zone of the equatorial Pacific upwelling zone. The concentrations of macronutrients are high, but phytoplankton biomass is low because grazing kept the dominant, relatively rapid-growing phytoplankton from increasing. The growth of rare, larger phytoplankton is limited by the availability of iron and grazing by mesozooplankton.

Nitrate and f_{CO_2} levels covaried, but CO_2 levels remained in excess and, even though the NO_3^- concentration was lower than historical values, there was no evidence for an important control on Δf_{CO_2} by the biological pump. A simple calculation shows that biological processes or gas exchange have little influence on the distribution of dissolved inorganic carbon and nitrogen. Assuming an upwelling velocity of 0.7 m day^{-1} and total inorganic carbon and nitrogen concentrations in upwelled water of 2000 mmol C m^{-3} and 3 mmol N m^{-3}, the total transport into the euphotic zone is 1400 mmol C m^{-2} day^{-1} and 2.1 mmol N m^{-2} day^{-1}. For comparison, primary production was about 100 mmol C m^{-2} day^{-1}, and loss of carbon by gas exchange, POC export, and DOC export were on the order of 2.5, 3, and 8 mmol C m^{-2} day^{-1}. Total carbon export was about 13.5 mmol C m^{-2} day^{-1}, and particulate nitrogen export was about 1.0 mmol N m^{-2} day^{-1}. Total export production from the equatorial Pacific zone for 1992 was about 1.2 Gt C year^{-1} (75% as DOC, 25% as POC). This is within the range of that originally estimated (*2*). Estimates of global ocean new production range from 5 to 20 GT C year^{-1} (*78*). Thus, assessing the global importance of this region is more uncertain. Only about 1.0% of upwelled carbon is exported by biological processes or is lost to the atmosphere. Most is simply exported horizontally by the vigorous physical circulation. Far more of it is exported by biological processes than is released to the atmosphere. In the case of nitrogen, the fraction involved in biological cycling may be as high as 25%, at least with the relatively low estimate of upwelling velocity given above. Physical, not biological, processes control the CO_2 flux in this region of the global system because biological cycling is so efficient that net flux out of the system is very small.

REFERENCES AND NOTES

1. R. H. Gammon, E. T. Sundquist, P. J. Fraser, in *Atmospheric Carbon Dioxide and the Global Carbon Cycle*, J. R. Trabalka, Ed. (DOE/ER-0239, U.S. Department of Energy, Washington, DC, 1985), pp. 25–62.
2. F. P. Chavez and R. T. Barber, *Deep-Sea Res.* **34**, 1229 (1987).
3. S. Chisholm and F. M. M. Morel, Eds., *Limnol. Oceanogr.* **36**, Preface (1991); J. J. Cullen, *ibid.*, p. 1578.

4. S. G. Philander, *El Niño, La Niña, and the Southern Oscillation* (Academic Press, San Diego, CA, 1990).
5. *U.S. GOFS Pacific Planning Report* (U.S. GOFS Report 9, U.S. Global Ocean Flux Study Planning Office, Woods Hole, MA, 1989). This project, EqPac, is part of a multination, multiyear international JGOFS effort in the Pacific Basin.
6. See J. W. Murray, M. W. Leinen, R. A. Feely, J. R. Toggwieler, R. Wanninkhof, *Oceanography* **5**, 134 (1992).
7. M. J. McPhaden and S. P. Hayes, *J. Geophys. Res.* **95**, 13195 (1990); M. Kubota and J. J. O'Brien, *ibid.* **93**, 13930 (1988); D. Herbert, J. N. Moum, D. R. Caldwell, *J. Phys. Oceanogr.* **21**, 1690 (1991).
8. Throughout this period, the equatorial Pacific was well instrumented with moored arrays of the Tropical Ocean Global Atmosphere–Tropical Atmosphere and Ocean Program (TOGA-TAO) and drifters of the Equatorial Pacific Ocean Climate Study (EPOCS).
9. Thirteen separate cruises were made consisting of 433 days of ship time on the R/V *Thompson*, R/V *Wecoma*, R/V *Baldrige*, and R/V *Discoverer*. Remote sensing data was collected on P-3B aircraft overflights. A set of meridional surveys was conducted from 12°N to 12°S at 170°, 140°, 125°, and 110°W. In October, the section at 170°W was moved to 95°W. Survey cruises from 12°N to 12°S at 140°W and 20-day time-series cruises at the equator at 140°W were conducted during February to May and during August to October, 1992. Moored deep sediment traps were deployed from January 1992 to January 1993, and a cruise focusing on benthic studies was conducted in November 1992 [J. McManus, *Eos* **74**, 180 (1993)].
10. M. J. McPhaden, *Oceanography* **6**, 36 (1993).
11. T. J. Conway *et al.*, *J. Geophys. Res.*, in press.
12. R. A. Feely *et al.*, *ibid.* **92**, 6545 (1987).
13. U. Siegenthaler, *Nature* **345**, 295 (1990). For example, during the 1986–1987 El Niño, the efflux of CO_2 was reduced to about 0.4 Gt C $year^{-1}$ [H. Inoue and Y. Sugimura, *Tellus B* **45**, 1 (1993)].
14. An additional complication for interpreting trends associated with the 1991–1992 El Niño are anomalies resulting from the June 1991 Mount Pinatubo eruption [R. A. Kerr, *Science* **263**, 1562 (1994)].
15. C. D. Keeling *et al.*, in *Aspects of Climate Variability in the Pacific and Western Americas*, D. H. Peterson, Ed. (Geophys. Monogr. Ser. 55, American Geophysical Union, Washington, DC, 1989), pp. 165–236.
16. A similar conclusion was reached with the use of coupled ocean circulation and carbon cycle models by A. M. E. Winguth *et al.* [*Global Biogeochem. Cycles* **8**, 39 (1994)].
17. J. L. Sarmiento, *Nature* **365**, 697 (1993).
18. R. A. Feely *et al.*, *Deep-Sea Res.*, in press. Gas exchange fluxes were calculated with use of the wind speed relations of R. H. Wanninkhof [*J. Geophys. Res.* **97**, 7373 (1992)].
19. T. S. Bates, K. C. Kelly, J. E. Johnson, *J. Geophys. Res.* **98**, 16969 (1993).
20. W. S. Kessler and M. J. McPhaden, *Eos* **73**, 280 (1992). These wind anomalies began around September 1991 and are manifestations of the Madden-Julian convective systems that form in the Indian Ocean, migrate to the Pacific Ocean, and die out near the date line (W. S. Kessler, M. J. McPhaden, K. M. Weickmann, *Deep-Sea Res.*, in press).
21. The scale of the east-west transport, which is proportional to the duration and intensity of the remote wind anomaly, calculated from the TOGA-TAO current meter data, is 5° to 10° longitude (W. Kessler, personal communication).
22. Correlation coefficient $r > 0.7$ with a 29-day time lag.
23. P.-M. Poulain, *J. Phys. Oceanogr.* **23**, 601 (1993).
24. K. Wyrtki, *ibid.* **11**, 1205 (1981).
25. R. A. Kerr, *Science* **262**, 656 (1993).
26. R. G. Najjar, J. L. Sarmiento, J. R. Toggweiler, *Global Biogeochem. Cycles* **6**, 45 (1992).
27. U. Siegenthaler and J. L. Sarmiento, *Nature* **365**, 119 (1993).
28. S. C. H. Philander, W. J. Hurlin, A. D. Seigel, *J. Phys. Oceanogr.* **17**, 1986 (1987).
29. M. J. R. Fasham, H. W. Ducklow, S. M. McKelvie, *J. Mar. Res.* **48**, 591 (1990).
30. J. R. Toggweiler, *U.S. JGOFS News* **2**, 1 (1990).
31. B. W. Frost and N. C. Franzen, *Mar. Ecol. Prog. Ser.* **83**, 291 (1992).
32. R. T. Barber, J. W. Murray, J. J. McCarthy, *Ambio* **23**, 62 (1994).
33. R. T. Barber and F. P. Chavez, *Science* **222**, 1203 (1983).
34. Chlorophyll integrated from depths of 0 to 120 m by J. Newton and J. W. Murray [*The Oceanography Society Third Scientific Meeting*, April 1993 (1993), p. 74].
35. Water for ^{14}C primary production was collected before dawn using a trace-metal clean sampling system. Samples were incubated for 24 hours in both an in situ array and a deck incubator with temperature and light quality control. R. T. Barber, M. L. Bender, J. J. McCarthy, *Eos* **73**, 281 (1992).
36. W. Gardner *et al.*, *Deep-Sea Res.*, in press.
37. Chlorophyll and P^B at the depth of the maximum primary productivity (P_{max}) are plotted here because their variability is maximal at P_{max}.
38. N. Lefevre and Y. Dandonneau, *Geophys. Res. Lett.* **19**, 2223 (1992).
39. R. A. Feely *et al.*, *ibid.* **21**, 277 (1994).
40. The front and patch were first observed from the National Aeronautics and Space Administration (NASA) overflights [J. A. Yoder, S. Ackelson, R. T. Barber, *Eos* **75**, 29 (1994)] and then on the R/V *Thompson*'s radar as the ship passed over the front during the night.
41. E. Johnson, personal communication.
42. D. E. Archer *et al.*, *Eos* **73**, 281 (1992).
43. E. T. Peltzer, *ibid.*, p. 287; H. W. Ducklow, H. L. Quinby, C. A. Carlson, *ibid.* **75**, 49 (1994); C. A. Carlson and H. W. Ducklow, *Deep-Sea Res.*, in press; E. T. Peltzer and T. Hayward, *ibid.*, in press.
44. R. B. Bacastow and E. Maier-Reimer, *Global Biogeochem. Cycles* **5**, 71 (1991).
45. These results are similar to those of R. T. Barber and J. H. Ryther [*J. Exp. Mar. Biol. Ecol.* **3**, 191 (1969)].
46. M. E. Ondrusek and R. R. Bidigare, *Eos* **73**, 287 (1992).
47. G. A. Fryxell, I. L. Iriarte, L. Duan, *The Oceanography Society Third Scientific Meeting*, April 1993 (1993), p. 70.
48. J. L. Iriarte and G. A. Fryxell, *Eos* **75**, 29 (1994).
49. R. R. Bidigare, *Deep-Sea Res.*, in press.
50. M. R. Landry, J. Constantinou, J. D. Kirshtein, *ibid.*, in press.
51. P. G. Verity, D. K. Stoecker, M. E. Sieracki, *Eos* **75**, 84 (1994).
52. H. G. Dam *et al.*, *Deep-Sea Res.*, in press; X. Zhang, H. G. Dam, J. R. White, M. R. Roman, *ibid.*, in press.
53. Compared with a similar study at the Bermuda JGOFS station [M. R. Roman, H. G. Dam, A. L. Gauzens, J. M. Napp, *Deep-Sea Res.* **40**, 883 (1993)], the equatorial Pacific has about 3 to 10 times higher primary production with a slightly lower mesozooplankton biomass.
54. J. W. Murray, J. Downs, S. Strom, C. L. Wei, H. Jannasch, *ibid.* **10**, 1471 (1989).
55. M. A. Peña, W. G. Harrison, M. R. Lewis, *Mar. Ecol. Prog. Ser.* **80**, 265 (1992); M. A. Peña, M. R. Lewis, J. J. Cullen, *J. Geophys. Res.* **99**, 14255 (1994).
56. R. C. Dugdale, F. P. Wilkerson, R. T. Barber, F. P. Chavez, *J. Geophys. Res.* **97**, 681 (1992).
57. N. M. Price, B. A. Ahner, F. M. M. Morel, *Limnol. Oceanogr.* **39**, 520 (1994).
58. S. Emerson, P. Quay, P. A. Wheeler, *Deep-Sea Res.* **40**, 2351 (1992).
59. P. A. Wheeler and S. A. Kokkinakis, *Limnol. Oceanogr.* **35**, 1267 (1990); P. A. Wheeler, *Eos* **73**, 281 (1992).
60. Q. Dortch, *Mar. Ecol. Prog. Ser.* **61**, 183 (1990).
61. P. R. Betzer *et al.*, *Deep-Sea Res.* **31**, 1 (1984).
62. J. Newton, T. Chapin, J. W. Murray, in preparation.
63. M. P. Bacon *et al.*, *Deep-Sea Res.*, in press.
64. K. O. Buesseler, J. E. Andrews, M. C. Hartman, R. Belastock, F. Chai, *ibid.*, in press.
65. J. W. Murray *et al.*, *ibid.*, in press.
66. K. O. Buesseler, M. P. Bacon, J. K. Cochran, H. D. Livingston, *ibid.* **39**, 1115 (1992).
67. E. T. Peltzer and P. G. Brewer, *Mar. Chem.* **41**, 243 (1993).
68. D. E. Harrison, *Deep-Sea Res.*, in press.
69. R. Wanninkhof *et al.*, *ibid.*, in press.
70. R. M. Gordon, K. H. Coale, K. S. Johnson, *Eos* **75**, 114 (1994).
71. E. Lindstrom *et al.*, *Nature* **330**, 533 (1987).
72. J. H. Martin, *ibid.* **353**, 123 (1991).
73. C. B. Miller *et al.*, *Oceanography* **4**, 71 (1991).
74. M. R. Roman *et al.*, *Deep-Sea Res.*, in press.
75. F. M. M. Morel, R. J. Hudson, N. M. Price, *Limnol. Oceanogr.* **36**, 1742 (1992); N. M. Price, L. F. Andersen, F. M. M. Morel, *Deep-Sea Res.* **38**, 1361 (1991).
76. R. M. Greene, Z. S. Kolber, D. G. Swift, N. W. Tindale, P. G. Falkowski, *Limnol. Oceanogr.* **39**, 1061 (1994); S. T. Lindley, R. R. Bidigare, R. T. Barber, *Deep-Sea Res.*, in press.
77. G. Arrhenius, in *The Sea*, M. N. Hill, Ed. (Interscience, London, 1963), vol. 3, p. 655; R. W. Murray and M. Leinen, *Geochim. Cosmochim. Acta* **57**, 4141 (1993).
78. W. M. Post *et al.*, in *Science of Global Change*, D. A. Dunnette and R. J. O'Brien, Eds. (ACS Symp. Ser. 483, American Chemical Society, Washington, DC, 1992), pp. 392–412.
79. R. T. Barber and F. P. Chavez, *Limnol. Oceanog.* **36**, 1803 (1991).
80. C. Garside, personal communication.
81. The CO_2 climatology was provided by T. Takahashi (personal communication).
82. P. Wheeler, personal communication.
83. D. Atwood, personal communication.
84. H. W. Ducklow, H. M. Quinby, C. A. Carlson, *Deep-Sea Res.*, in press; D. Kirchman, J. Rich, R. T. Barber, *ibid.*, in press.
85. A. J. White *et al.*, *ibid.*, in press.
86. C. Goyet, personal communication.
87. F. Chavez, personal communication.
88. Logistical support for the EqPac project was provided by NSF OCE 9024379 and the NOAA Climate and Global Change Program. For continuous support, we thank N. Andersen, P. Taylor, M. Scott, L. Duguay, and J. Todd. We thank the captains, crews, and technicians of the R/V *Thompson*, R/V *Baldridge*, and R/V *Discoverer* for help; S. Kadar for logistical support; and B. Frost, K. Banse, and L. Balistrieri for reviewing the manuscript. We thank all of the EqPac investigators who have contributed data and ideas. Some of the ideas presented here reflect discussions held at two JGOFS/EqPac workshops. This paper is University of Washington School of Oceanography contribution number 2009, Pacific Marine Environmental Laboratory contribution number 1461, University of Maryland Center for Environmental and Estuarine Studies contribution 2552, and US-JGOFS contribution number 107.